DISPLACEMENT IN THE TURBULENT BOUNDARY LAYER ON A PERMEABLE PLATE WITH SUPERCRITICAL INJECTION

S. A. Druzhinin, A. A. Zelengur, V. N. Mamonov, and B. P. Mironov

Zhurnal Prikladnoi Mekhaniki i Tekhnicheskoi Fiziki, Vol. 10, No. 1, pp. 112–116, 1969

The displacement thickness in a turbulent boundary layer is determined for supercritical injection parameters. Experimental relations between the displacement thickness and the injection parameter are obtained for air, helium, and freon-12 injected into air.

The turbulent boundary layer with transverse mass addition is encountered in many practical problems such as the protection of structural elements, combustion, etc. Of most interest are regimes in which the value of the injection parameter is critical:

$$b = \frac{\rho_w v_w}{\rho_0 u_0} \frac{2}{cf_0} = b_*$$

Here, cf_0 is the coefficient of friction under standard conditions; ρ_w and ρ_0 are the densities of the injected gas and the main stream; v_w is the velocity of the injected gas at the wall; and u_0 the flow velocity at the outer edge of the boundary layer.

In this case, in accordance with [1,2], the main stream begins to be pushed away from the porous surface. There have been a number of experimental investigations of this flow region [3,4]. The investigation of the turbulent boundary layer at supercritical injection parameters ($b > b_*$) is also of considerable interest. In [5,6] the hydrodynamics of this regime were investigated and the existence of a displacement layer observed [6].

The so-called displacement thickness δ' is the thickness of a certain layer at the wall, characteristic of supercritical injection, in which the velocity component is equal to zero.

We have conducted experiments in a subsonic wind tunnel with a working section measuring 100 × 120 mm at a maximum air flow velocity of 70 m/sec.

In the upper wall of the working section we installed a porous plate of stainless steel measuring 600 × 70 × 5 mm with a porosity of 30% (mean pore diameter 10 μ) consisting of three individual sections. In order to ensure zero-gradient flow the bottom wall of the working section was made movable. Provisions were made for heating the main stream and the injected gas. By using an IAB-451 Töpler instrument with an anamorphic attachment we were able to make visual observations of the boundary layer. The boundary layer was not sucked off before the beginning of the porous plate; accordingly, during the experiments we measured the initial momentum thickness ahead of the porous plate. The velocity profile was measured with a rectangular microtube measuring 1.5 × 0.5 mm.

The displacement thickness was measured with two hot-wire anemometers, whose readings were recorded by means of an N-700 loop oscillograph. The anemometer probe was a gold-plated tungsten filament 8 μ in diameter and 5 mm long secured in a holder. The distance between the probe and the wall was measured with a KM-6 cathetometer correct to ±0.005 mm. The point of contact of the probe with the surface was determined optically from the superposition of the probe and its reflection at the porous surface. When the injected gas was different from the main-stream gas, the concentration profile was measured with a GSTL-3 gas analyzer correct to ±3%. The flow rate of injected gas was measured correct to ±3% with double orifice plates.

The preliminary part of the experiment consisted of investigating the development of the boundary layer on the porous plate with and without injection. These experiments revealed the presence of a fully developed turbulent boundary layer on the porous plate.

In conducting the experiments it was noted that at supercritical injection parameters a layer in which there are no fluctuations of the velocity vector exists at the porous wall. As measurements showed, the zone in which there are no velocity fluctuations coincides with the zone in which the longitudinal velocity component is equal to zero, i.e., with

the thickness of the displacement layer. At the same time, the boundary of this layer is quite sharply expressed in relation to the velocity fluctuations and easily determined, whereas determining it from longitudinal velocity measurements presents certain difficulties associated both with the measurement of the velocity near the wall and with the precise location of the boundary.

The displacement thickness was measured as follows.

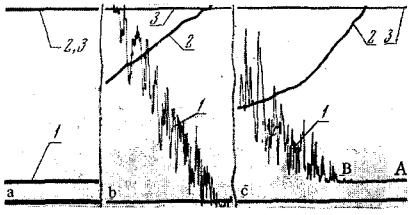

Fig. 1. Typical oscillograms: a — $u_0 = 0$, $\rho_w v_w \neq 0$; b — $u_0 \neq 0$, $\rho_w v_w = 0$; c — $u_0 \neq 0$, $\rho_w v_w \neq 0$, 1) trace of anemometer readings near the wall, 2) trace of velocity in flow core, 3) base line.

The anemometer probe was positioned at a certain distance from the permeable surface. Gas was injected through the porous plate at a constant rate in the absence of the main stream, which corresponded to the regime $b \to \infty$. In this case, of course, the anemometer wire was located in the displacement layer, which enabled us to make reliable measurements of the velocity fluctuations typical of this layer. The main stream was then switched on and its velocity increased smoothly from 10 to 60 m/sec. This was accompanied by a reduction in the thickness of the displacement layer and at a certain instant the displacement boundary intersected the anemometer probe. At this instant the anemometer registered intense velocity fluctuations. The velocity of the main stream was measured with a second hot-wire anemometer, whose probe was inserted into the flow core. A typical oscillogram of the process is shown in Fig. 1c. It is clear from the oscillogram that on the interval AB (curve 1) the anemometer probe is located in the displacement layer, since there are no velocity fluctuations and the velocity itself is constant, despite a considerable increase in the main-stream velocity (curve 2). On the interval BC the absolute value of the velocity and, in particular, its fluctuations sharply increase. This justifies us in taking the zone around point B as the displacement boundary. For comparison, Fig. 1a,b presents oscillograms obtained with the probe at the same distance from the porous surface as in the previous case for $\rho_w v_w \neq 0$, $u_0 = 0$ (a) and for $\rho_w v_w = 0$, $u_0 \neq 0$ (b), while Fig. 2 shows photographs of the velocity vector fluctuation spectra in (a) and outside (b) the displacement layer in the frequency range 20–500 Hz, obtained with an SK4-3 frequency spectrum analyzer.

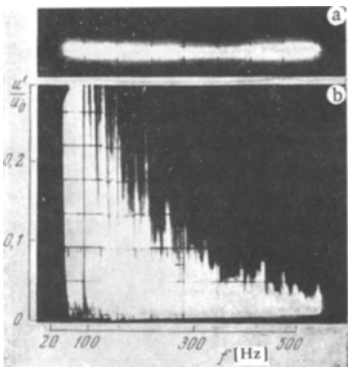

Fig. 2. Velocity vector fluctuation spectra in the range 20–500 Hz: a) in the displacement layer, b) outside the displacement layer.

The displacement thickness was measured at both increasing and decreasing values of the main-stream velocity. The results obtained for these two cases coincide.

The so-called "wall effect" [7] did not affect the correctness of determination of the displacement thickness, since during the experiment the anemometer probe was located at a constant distance from the wall and used only to register the occurrence of velocity fluctuations.

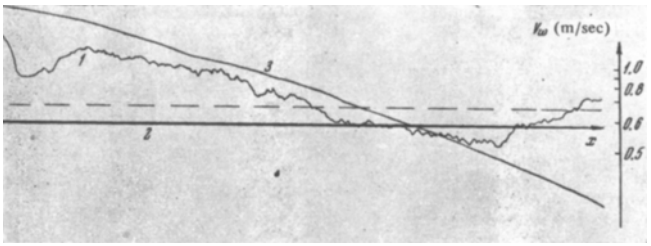

Fig. 3. Oscillogram of the permeability of an experimental specimen: $\langle \rho_w v_w \rangle = 119.8$ N/m^2 · sec, $\langle v_w \rangle = 0.66$ m/sec; 1) injected gas velocity, 2) base line, 3) longitudinal coordinate; broken line-mean-Flow injection velocity.

Before carrying out the principal experiments, we checked the permeability of the porous specimens with a hot-wire anemometer. Gas was passed through the porous specimen at a constant rate, and the anemometer probe was moved along the specimen at a distance of 0.5 mm from the surface. The coordinate of the probe along the length of the plate and the anemometer signal were recorded on a loop oscillograph. Preliminary calibration made it possible to determine the velocity of the injected gas at any point of the porous plate from the oscillogram obtained (Fig. 3).

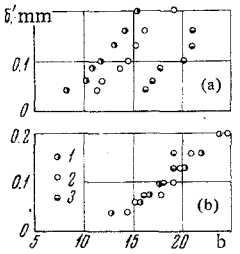

Fig. 4. a) Analysis based on mean flow injection velocity; b) analysis based on local injection velocity; the points 1, 2, and 3 correspond to the values v_W = = 0.51, 0.43, 0.30 m/sec and $\langle v_W \rangle$ = 0.33 m/sec.

As the measurements showed, injection was significantly nonuniform along the length of the specimens. Since the velocity of the injected gas v_W enters into the expression for the injection parameter b, it was necessary to establish the effect of this nonuniformity on the relation $\delta' = f(b)$. In Fig. 4a we present the results of measurements of displacement thickness in several cross sections with different local injection volocities, the quantity b being determined from the mean velocity $\langle v_W \rangle$. As may be seen from the graph, the experimental points diverge considerably. In Fig. 4b the same experimental data are shown, but this time the parameter b has been determined from the local injection velocity. Clearly, in this case all the points are grouped about a single curve.

Accordingly, all the subsequent experimental data on the displacement thickness were analyzed according to the local injection velocity and the measurements were made at the same cross section (x = 310 mm from the beginning of the porous plate) selected from considerations of injection uniformity. In this section the ratio $v_W/\langle v_W \rangle = 1.54$ and remained constant at different values of $\langle v_W \rangle$ correct to 4%.

The results of experiments to measure the displacement thickness of helium, air, and freon-12 injected into air on the range u_0 = 10–60 m/sec are presented in Fig. 5 in the form:

$$R' = f(b) \quad \left(R' = \frac{u_0 \delta'}{\nu}\right)$$

The coefficient of friction C_{f_0} for calculating b was determined from the formula:

$$1/2 C_{f_0} = 0.0126\,(R^{**})^{-0.25} \tag{1}$$

Here, the values of R** were found experimentally by measuring the velocity and concentration profiles in the section where the anemometer probe was located.

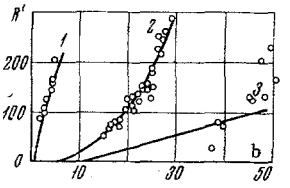

Fig. 5. Reynolds number R' as a function of injection parameter; 1) injection of helium into air $\rho_W v_W$ = 16.55 N/m^2 · sec; 2) injection of air into air $\rho_W v_W$ = 59.2, 86.8, 119.8 N/m^2 · sec; 3) injection of freon-12 into air $\rho_W v_W$ = 181.5 N/m^2 · sec; curves represent calculations based on equation (4).

The need to introduce these coordinates for analyzing the experimental data in the form R' = f(b) follows not only from the nature of the experimental material but also from the theoretical considerations outlined below.

The value of δ' can be approximately estimated if it is assumed that for supercritical injection the following relations hold (correct to the coefficient):

$$\delta' = A \frac{\rho_w v_w^2}{\rho_0 u_0^2} (x - x_*) \tag{2}$$

which follows from the boundary condition for two colliding jets, and

$$\frac{d\delta^{**}}{dx} = \frac{\rho_w v_w}{\rho_0 u_0} \tag{3}$$

which follows from the momentum equation for supercritical injection. Here, x_* is the distance from the beginning of the boundary layer to the point at which displacement begins, and x is the distance from the beginning of the boundary layer to the section in question.

Using (1)–(3), we obtain an expression for the Reynolds number

$$R' = A \frac{\rho_0}{\rho_w} \frac{(0.0126)^4}{(\rho_w v_w / \rho_0 u_0)^3} \left[\left(\frac{\rho_w v_w}{\rho_0 u_0} \frac{2}{C_{f_0}}\right)^4 - b_*^4\right] \tag{4}$$

The relation R' = f(b) calculated from Eq. (4) with A = 1 is presented in Fig. 5. In accordance with [1, 2], the values of b_* for curves 1, 2, and 3 have been taken as 1, 5, and 10, respectively.

In the calculations the relations R' = f(b, $\rho_W v_W/\rho_0 u_0$) or b = f (R', $\rho_W v_W/\rho_0 u_0$) were found from the experimental values of the parameters. Equation (4) should be regarded as approximate, since there are discrepancies between the theoretical and experimental data (for example, curve 3).

It is interesting to compare the experimental results in the form $b_i/b_0 = f(M/M_0)$ (Fig. 6) for the injection of helium and freon-12 into air in supercritical regimes at R' = idem with the theoretical relation $b_{i*}/b_{0*} = f(M/M_0)$ for the critical values presented in [1, 2]. Here, b_i and b_0 are the values of the injection parameters for the injection of gas i into air and air into air at R' = idem from Fig. 5; b_{i*}, b_{0*} are the values of the critical injection parameters for the injection of gas i into air and air into air; M and M_0 are the molecular weights of the injected gas and the main-stream

gas.

Clearly, the ratio of the supercritical injection parameters as a function of the ratio of the molecular weights of the injected and main-stream gases is in satisfactory agreement with the theory for the critical injection parameters.

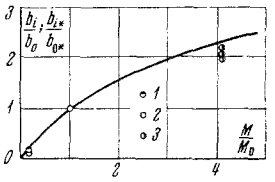

Fig. 6. Relative injection as a function of the ratio of the molecular weights of the injected and main-stream gases; 1) injection of helium into air; 2) injection of air into air; 3) injection of freon-12 into air.

At the same time, we made visual observations of the boundary layer with an IAB-451 Töpler instrument using an anamorphic attachment that gave a relative magnification of the vertical coordinate of 10:1 with respect to the horizontal coordinate.

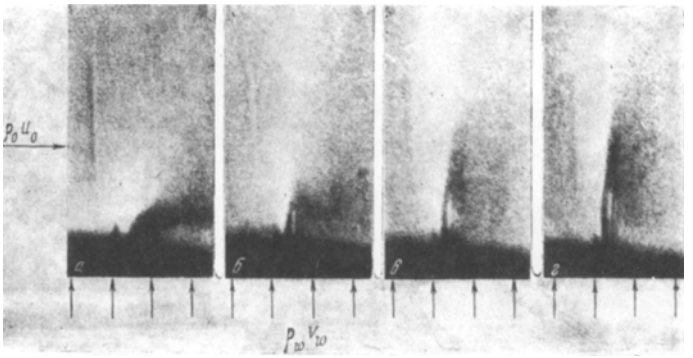

Fig. 7. Photographs of the thermal wake behind a heated wire obtained by the schlieren method with an anamorphic attachment; frames a, b, c, and d correspond to the values b = 3.6, 12.8, 17.7, and 19.4.

An electrically heated nichrome wire 0.1 mm in diameter was stretched over the porous surface at right angles to the flow and the thermal wake was observed. Photographs of the wake are shown in Fig. 7.

In Fig. 7b, c, d there is a clearly visible zone of intense blowing at the wall (vertical black streak), corresponding to a zero value of the longitudinal velocity component, which increases with increase in the injection parameter. For comparison, Fig. 7a shows a photograph of the thermal wake at $b < b_*$, from which it is clear that there is no zone of zero longitudinal velocity component near the wall.

A similar picture was observed in [6].

REFERENCES

1. S. S. Kutateladze and A. I. Leont'ev, Turbulent Boundary Layer of a Compressible Gas [in Russian], SO AN SSSR, Novosibirsk, 1962.

2. Heat Transfer and Friction in the Turbulent Boundary Layer [in Russian], In-t Teplofiziki, SO AN SSSR, Novosibirsk, 1964.

3. A. I. Leont'ev, B. P. Mironov, and P. P. Lugovskoi, "Experimental determination of critical injection on a porous plate," Inzh.-fiz. zh. [Journal of Engineering Physics], vol. 10, no. 4, 1966.

4. P. P. Lugovskoi and B. P. Mironov, "Effect of positive longitudinal pressure gradient on critical injection parameter," Inzh.-Fiz. zh [Journal of Engineering Physics], vol. 13, no. 4, 1967.

5. V. P. Mugalev, "Experimental investigation of the subsonic turbulent boundary layer on a plate with blowing," Izv. VUZ. Aviatsionnaya tekhnika, no. 3, 1959.

6. D. S. Hacker "Interferometric investigation of the stability of a turbulent boundary layer with mass addition," ASME Paper no. 58-A-249.

7. A. B. Wills, "The correction of hot-wire readings for proximity to a solid boundary," J. Fluid Mech., 12, 3, 1962.

13 August 1968

Novosibirsk